SI Appendix

Materials and Methods

Plant materials and growth conditions

Arabidopsis thaliana (L.) Heynh. ecotype Col-0 wild-type and transgenic plants were grown in soil containing the mixture of peat moss and perlite (1:1), under a 16-h photoperiod at 22°C in a greenhouse with 20 to 30% humidity. The *atabcg28* knockout mutants *atabcg28-1* (GK-372E03) and *atabcg28-2* (GK-401E01) were obtained from the GABI-Kat collection (1). The *atnap12* knockout mutants *atnap12-1* (SAIL-776G03) and *atnap12-2* (SALK-104924) were obtained from SAIL and SALK, respectively (2). The T-DNA insertion sites of these mutants are presented in SI Appendix, Figure S2. The T-DNA insertion was validated by genomic DNA-PCR and sequencing. CS8846 (*qrt1-2* in the Col-3 background) was obtained from the Arabidopsis Biological Resource Center (3).

Transgenic plant generation

The plasmid constructs used to generate transgenic plants are summarized in SI Appendix, Fig. S3 and primer information for the constructs is provided in SI Appendix, Table S2. The constructs were introduced into Arabidopsis plants using *Agrobacterium tumefaciens* (strain GV3101)–mediated floral dipping (4). Transgenic plants were selected on ½ MS supplemented with hygromycin (20 mg/L) for the pCambia1300 backbone, and kanamycin (30 mg/L) for the pBI121 and pMDC100 backbones. For the complementation test shown in Table 1, the T2 seeds of 14 independent transgenic *atabcg28-1*/+ lines and 9 *atabcg28-2*/+ lines that were transformed with *gAtABCG28* were sown in ½ MS medium containing 5 μg/mL sulfadiazine. The segregation ratio of all tested lines ranged from 1:1.8 to 1:3.2, which was significantly different from the 1:1 ratio of *atabcg28*/+. Five representative complementation lines per T-DNA insertion background are presented in Table 1.

Histochemical staining of pollen

For the *promoter-GUS* expression assay, flowers and developing siliques of pAtABCG28::GUS plants (T2) were stained with GUS staining solution as described (5)

and cleared with 2 M NaOH solution. Twenty-one out of 27 independent transgenic lines tested exhibited a pAtABCG28::GUS signal in mature pollen and pollen tubes. To observe pollen development, dehydrated flower buds at various stages of development were embedded in Technovit 7100 (Kulzer) and serially sectioned (10-μm thickness) using a Leica RM2245 rotary microtome. Sectioned samples were stained with Toluidine Blue as described (6). For a pollen viability test, the whole anther of *atabcg28*/+ *qrt1* was stained with Alexander staining solution (7). To stain vacuoles, *atabcg28*/+ tetrad pollen grains were soaked in 0.02% (w/v) neutral red for 30 min as described (8).

Analysis of the effect of polyamines on root hair growth and ROS generation

T3 homozygous lines of pEXPA7::EYFP:AtABCG28 were grown on ½ MS with agar (1.5%) for 5 days. Seedlings of similar size were transferred to 1/8 MS media (MES 2.5 mM), of various pH values with or without 0.175 mM Spermine (Sigma-Aldrich, Cat. No. S3256) and with or without 25 or 50 μM polyamine oxidase inhibitor MDL72527 (Sigma-Aldrich, Cat. No. M2949) on glass microscopy slides and covered with cover glasses. Root hair growth was observed 36–48 h after transfer.

To observe ROS, 1/8 MS medium containing 5 μM CellROX® Deep Red Reagent (Invitrogen™, Cat. No. C10422) was applied to the slide containing whole seedlings. After 30 minutes of staining at room temperature, the staining dye was washed out three times with 1/8 MS medium. ROS in root hairs of newly grown roots were visualized and quantified based on intensity of the signal as described below. CellROX® Deep Red Reagent has the highest sensitivity for hydroxyl radical (Invitrogen).

Cloning and plasmid construction

For the complementation test, the ~6.6-kb genomic region of *AtABCG28* including the promoter was cloned into a pCambia 1300 vector. To generate mGFP4 or EYFP-tagged AtABCG28, the mGFP4 or EYFP coding sequence (CDS) was inserted in-frame right after the signal peptide of either *AtABCG28* genomic DNA without a promoter or the coding sequence. For overexpression of *AtABCG28* in pollen tubes and root hairs, *AtABCG28* expression was driven by the pollen-specific LAT52 promoter (9) and the epidermis-specific EXPANSIN 7A promoter (10), respectively, as described (11).

The native full-length CDS of AtABCG28 was structurally unstable in bacteria. Therefore, to generate a structurally stable CDS, several sense mutations were introduced to prevent formation of a hairpin loop structure (Figure S9). Site-directed mutagenesis was performed as described (12). Information about primers used for cloning is available in Table S2.

Microscopy observations

Images of GUS staining and root hairs were taken using an Olympus SZX 12 microscope and Nikon Digital Camera DXM1200F. Fluorescent images of AtABCG28 subcellular localization, ROS, and polyamines were acquired by confocal laser scanning microscopy (CLSM) using Zeiss LSM510 META and Olympus BX51 microscopes.

Time-lapse images of ROS in germinating pollen tubes stained with CM-H_2DCFDA were acquired using an Olympus DSU-IX81 spinning disc confocal microscope with a 63×/1.40 NA DIC oil immersion objective. Microscopy settings were described previously (13). Pollen grains and tubes were imaged every 1 min over a 30-min period in z-stacks of 12 optical slices. CM-H_2DCFDA and pentafluorobenzenesulfonyl fluorescein-stained pollen were excited with a 488-nm laser and emission signals were detected at 505–545 nm. CellROX® Deep Red reagent-treated samples were excited with a 633-nm laser and emission signals were detected at wavelength longer than 655 nm. For simultaneous detection of EYFP and FM4-64, samples were excited with 488- and 543-nm lasers, respectively, with the dichroic mirrors set to DM 488/543/633. Fluorescence signals were detected at 500–530 nm for EYFP and 600–700 nm for FM4-64.

Quantification of ROS and polyamine distribution

Intensity profiles were generated by measuring the fluorescence intensity of DCFH_2-DA (for ROS detection) or Alexa Fluor 568 (for polyamine detection) along the longitudinal axis of the pollen tube from the very tip to 5 μm away from the tip using ImageJ (14). To measure the ratio of fluorescence intensities (I tip/I grain), mean fluorescence intensity values from the tip were divided by those measured from a region inside the grain (5–7 μm from the tip). ROS in the root epidermis of Col-0 and *AtABCG28*-expressing plants were measured using ImageJ. The fluorescence intensity was calculated as the corrected

total cell fluorescence (CTCF). CTCF = integrated density – (area of selected cell × mean fluorescence of background readings).

Graph and statistical analyses

Graph and statistical analyses were performed using GraphPad Prism 5. Statistical significance was calculated using a Chi-square test, two-way ANOVA and Bonferroni post-tests, and an unpaired *t* test.

Table S1. **Complementation of the male fertility defect in *atabcg28* by introducing the *pAtABCG28::mGFP4:gAtABCG28* or *pLAT52::EYFP:gAtABCG28* constructs into the heterozygous *atabcg28*$^{-/+}$ T-DNA insertion mutant (*atabcg28-2*$^{-/+}$).** Among the progeny of homozygous *pAtABCG28::mGFP4:gAtABCG28* or *pLAT52::EYFP:gAtABCG28* transgenic plants, homozygous *atabcg28*$^{-/-}$ could be isolated, and the transmission of heterozygous *atabcg28*$^{-/+}$ followed approximately the 3:1 ratio expected for Mendelian inheritance.

Line	Self-fertilized progeny					Expected genotype of the parent plant
	Sul ^{R} *atabcg28*$^{-/+}$ and *atabcg28*$^{-/-}$	Sul ^{S} +/+ (WT)	Segregation ratio	X^2	P value	
9-3	45	22	2 : 1	11.56	< 0.001	*atacbg28*$^{-/+}$; *mGFP4:gAtABCG28*$^{+/+}$
9-8	69	0	1 : 0	100	< 0.0001	*atacbg28*$^{-/-}$; *mGFP4:gAtABCG28*$^{+/+}$
9-12	123	0	1 : 0	100	< 0.0001	*atacbg28*$^{-/-}$; *mGFP4:gAtABCG28*$^{+/+}$
9-13	56	23	2.4 : 1	17.64	< 0.0001	*atacbg28*$^{-/+}$; *mGFP4:gAtABCG28*$^{+/+}$
10-1	159	0	1 : 0	100	< 0.0001	*atacbg28*$^{-/-}$; *mGFP4:gAtABCG28*$^{+/+}$
10-7	50	17	2.9 : 1	25	< 0.0001	*atacbg28*$^{-/+}$; *mGFP4:gAtABCG28*$^{+/+}$
10-16	110	0	1 : 0	100	< 0.0001	*atacbg28*$^{-/-}$; *mGFP4:gAtABCG28*$^{+/+}$
3-4	88	0	1 : 0	100	< 0.0001	*atacbg28*$^{-/-}$; *EYFP:gAtABCG28*$^{+/+}$
3-5	103	0	1 : 0	100	< 0.0001	*atacbg28*$^{-/-}$; *EYFP:gAtABCG28*$^{+/+}$
3-7	101	43	2.3 : 1	16.00	< 0.0001	*atacbg28*$^{-/+}$; *EYFP:gAtABCG28*$^{+/+}$
2-9	90	0	1 : 0	100	< 0.0001	*atacbg28*$^{-/-}$; *EYFP:gAtABCG28*$^{+/+}$
2-10	63	25	2.5 : 0	19.360	< 0.0001	*atacbg28*$^{-/+}$; *EYFP:gAtABCG28*$^{+/+}$
2-12	85	0	1 : 0	100	< 0.0001	*atacbg28*$^{-/-}$; *EYFP:gAtABCG28*$^{+/+}$
***atabcg28-2*$^{-/+}$**			**1 : 1**			

The genomic fragment of *AtABCG28* was used to generate the *pAtABCG28::mGFP4:gAtABCG28* and *pLAT52::EYFP:gAtABCG28* construct. Genotypes of progeny were determined based on resistance to sulfadiazine. The sulfadiazine selection system was used to generate the original T-DNA insertional mutant *atabcg28-2*$^{-/+}$ (https://www.gabi-kat.de/). P values < 0.001 and < 0.0001 indicate a significant difference from the 1:1 segregation ratio of transmission defect in *atabcg28-2*$^{-/+}$, calculated using a Chi-square test. T3 generation seeds of homozygous *pAtABCG28::mGFP4:gAtABCG28* or *pLAT52::EYFP:gAtABCG28* transgenic plants were used in this analysis. Sul ^{R}, sulfadiazine resistant; Sul ^{S}, sulfadiazine sensitive.

Table S2. Primers used in this study

Purpose and primer name	Primer sequence (5'-3')	Reference
***atnap12* genotyping**		
SAIL_LB3	TAGCATCTGAATTTCATAACCAATCTCGATACAC	https://www.arabidopsis.org/abrc/sail.jsp
F1	TTGGGTTGATGCTGAGAGTAG	
R1	TGCGCTAAATCGAAGGTTCTC	
SALK_LBb1.3	ATTTTGCCGATTTCGGAAC	http://signal.salk.edu/
F2	AACTACATTTCTTTCTGCCTTGG	
R2	TCGTTCACCTTCGCAAGAG	
***atabcg28* genotyping**		
GABI 8474	ATAATAACGCTGCGGACATCTACATTTT	https://www.gabi-kat.de/
F3	TCCGCCTGATTACTACATTGA	
R3	GGGAACGTAA AGCTACTTCT TT	
pCambia1300-pAtABCG28::AtABCG28 (Complementation)		
Pro-F-NarISalI	GGCGCCGTCGACCCAATGGCCTTCAAAACTG	
gAtABCG28-KpnI-R	GGTACGCTTGAAGGTTTCTCATTGCTTC	
pBI121-pAtABCG28::GUS (GUS)		
Pro-GUS-HindIII-F	AAGCTT CCAATGGCCTTCAAAACTG	
Pro-GUS-BamHI-R	GGATCC CCCTGAAAATTTTCCAAGAAA	
pMDC100-pLAT52::EYFP:gAtABCG28 (Overexpression)		
pLAT52-F	AAGCTTGCATGCCTGCAGGTCGAC	(9, 15)
pLAT52-R	TGAAATCCTTCAATCGAATTC	
pMDC100-pEXPA7::EYFP:AtABCG28-CDS-SDM (Ectopic expression)		
pEXPA7-F	ATTAGGGTCCAAGGTTGTTC	(11)
KpnI-pEXPA7-R	GGTACCTCTAGCCTCTTTTTCTTTATTC	
28-CDS-F	ATGGGAAGGAGAAATTCATATT	
28-CDS-R	GAACGTAAAGCTACTTCTT	
Site-directed mutagenesis		
28CDS-hairpin rev-F2	TGTAGATTGCCAGCTGATCTCCCAAAGCCGGAGAAA	
28CDS-hairpin rev-R2	ATCAGCTGGCAATCTACATCTTGCGCTGAACCAAAG	
N-SacI-Linker-EYFP-F	GAGCTCGGAGGTGGAGGTGGAGCTATGGTGAGCAAGGGCGAG	
C-SacI-Linker-EYFP-R	GAGCTCAGCACCAGCAGCAGCAGCAGCTCCAGCCTTGTACAGCTCGTCCATGCC	

Supplementary Information Figures

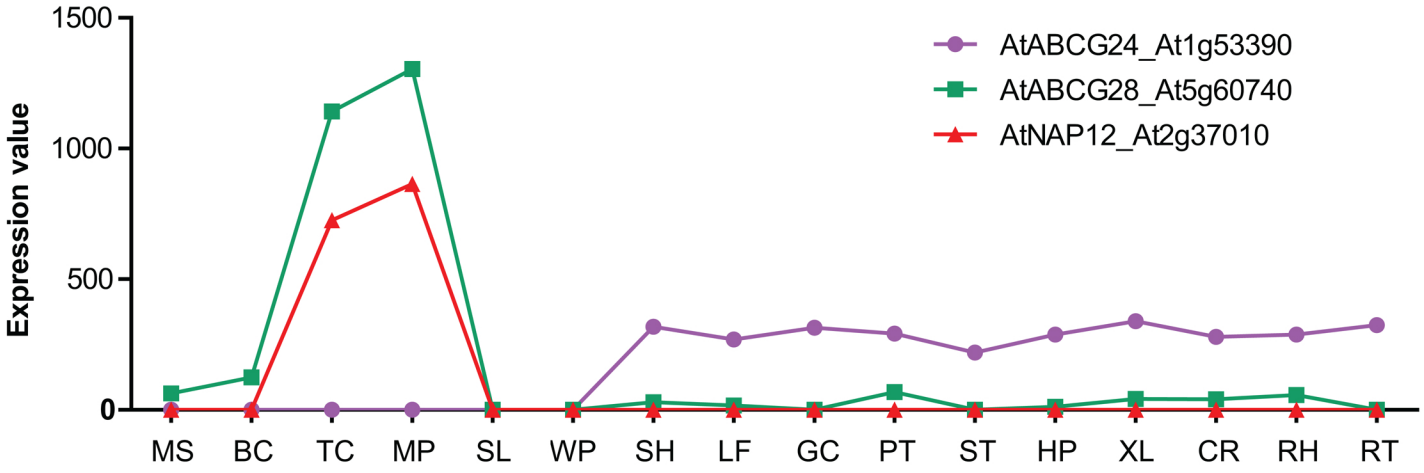

MS = Microspore
BC = Bicellular pollen
TC = Tricellular pollen
MP = Mature pollen

SL = Seedlings
WP = Whole plants
SH = Shoots
LF = Leave

GC = Guard cell-enriched leaf extracts
PT = Petioles
ST = Stems
HP = Hypocotyls

XL = Xylem
CR = Cork
RH = Root hair zone
RT = Roots

Figure S1. *AtABCG28* and *AtNAP12* are specifically expressed in tricellular stage and mature pollen grains.
Expression values of NAP12-like subfamily members were obtained from from ref 16 (Bock et al., 2006).

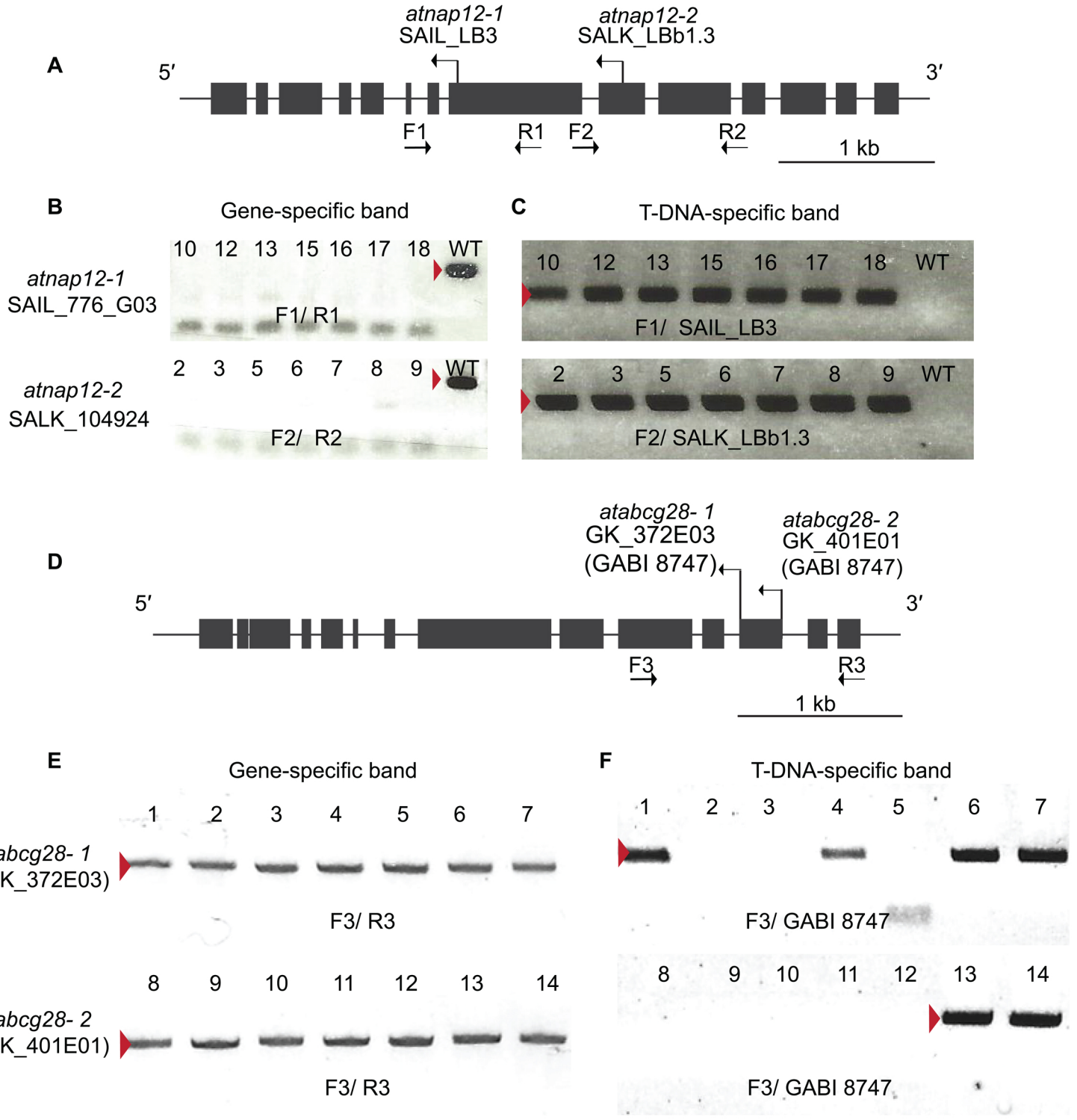

Figure S2. Genotyping of T-DNA-insertional mutants of *atnap12* and *atabcg28* revealed that *atnap12* mutants can be self-fertilized to produce homozygous progeny, whereas *atabcg28* mutants cannot.

(A, B, and C) Genotyping of *atnap12-1* (SAIL_776G03) and *atnap12-2* (SALK_104924). T-DNA insertion sites of *atnap12-1* and *atnap12-2* (A). Primer pairs F1/R1 (SAIL_776G03) and F2/R2 (SALK_104924) were used to amplify *AtNAP12*, with a target size of 1317 bp (B). T-DNA-specific bands for SAIL_776G03 and SALK_104924 were amplified using the primer set F1/ SAIL_LB3, with a predicted band size larger than 473 bp and F2/SALK_LB1.3, with a predicted band size larger than 528 bp (C).

(D, E and F) Genotyping of *atabcg28-1* and *atabcg28-2* in the *quartet 1* (*qrt1*) background. T-DNA insertion sites of *atabcg28-1* and *atabcg28-2* (D). An *AtABCG28*-specific band was amplified using the F3/R3 primer set, with a predicted band size of 1482 bp (E). T-DNA insertion bands for *atabcg28-1* (GK_372E03) and *atabcg28-2* (GK_401E01) were amplified using F3/GABI 8747 (F). The expected T-DNA-specific band size was 894 bp and 1107 bp, respectively. The validity of the amplified bands was checked by sequencing.

Boxes, exons. Lines, introns. Arrows show the position and direction of T-DNA insertion, and the direction of forward (F) and reverse (R) primers. Red arrowheads indicate bands of the expected size.

Figure S3. Diagrams of constructs used.
(A) Construct used for complementation with a whole genomic fragment of *AtABCG28* (*gAtABCG28*).
(B) Promoter GUS construct.
(C) Construct used to localize *AtABCG28* expression using a genomic fragment of *AtABCG28* under the control of its endogenous promoter *pAtABCG28*. The coding sequence of *mGFP4* was fused in-frame after the sequence encoding a predicted signal peptide of *AtABCG28*. Two linker sequences between mGFP4 (green) and AtABCG28 are indicated. SP, signal peptide (red); A, Alanine; G, Glycine.
(D) Construct used to localize *AtABCG28* expression using a genomic fragment of *AtABCG28* under the control of the pollen-specific promoter *LAT52*. The coding sequence of *EYFP* was fused in-frame after the sequence encoding a predicted signal peptide of *AtABCG28*. *EYFP* insertion strategy is similar to that shown in (C) for *mGFP4*.
(E) Construct for ectopic expression of *AtABCG28* in root hairs using a site-directed mutagenized coding sequence of *AtABCG28 (CDS-SDM)* driven by the *EXPANSIN 7A* promoter. Strategy for site-directed mutagenesis is explained in Fig. S9. *EYFP* insertion strategy is similar to that shown in (C) for *mGFP4*.

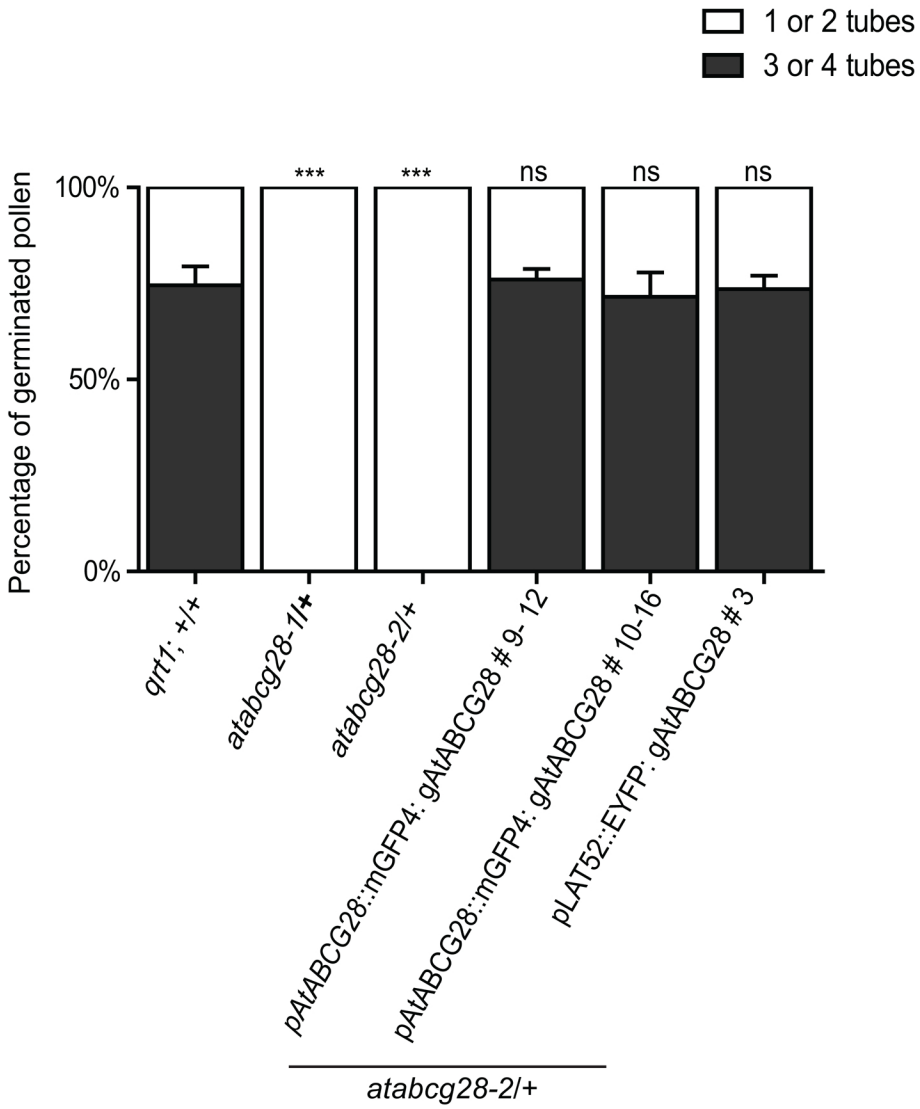

Figure S4. *pAtABCG28::mGFP4:AtABCG28* and *pLAT52::EYFP:gAtABCG28* complemented the pollen tube growth defect in *atabcg28*/+.

Percentage values of tetrads with germinated pollen tubes in the *qrt1* background control, *atabcg28*/+ lines, *atabcg28*/+ lines complemented with *mGFP4:AtABCG28* expressed under its endogenous promoter (Lines 9-12 and 10-16), or *EYFP:AtABCG28* expressed under the pollen overexpressing *pLAT52* promoter (Line 3). Error bars are standard deviation (SD). Data were obtained from 200 to 400 tetrads per genotype in two independent experiments. Asterisks denote statistically significant differences between the *qrt1* background control and transgenic plants, calculated by two-way ANOVA and Bonferroni post-tests (***, $p < 0.001$; ns (not significant), $p > 0.05$).

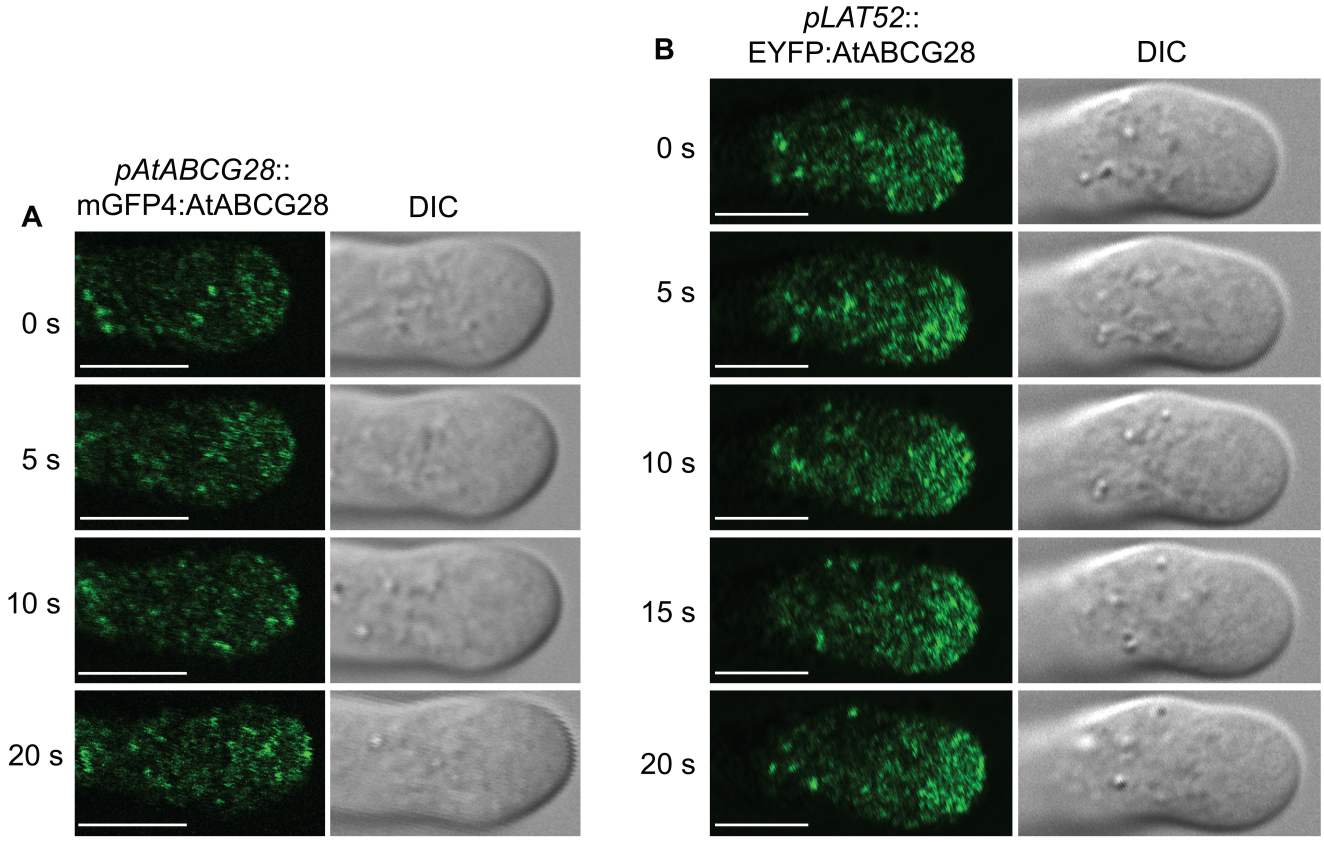

Figure S5. The localization patterns of fluorescence-tagged AtABCG28 did not differ between pollen tubes expressing *AtABCG28* driven by its endogenous promoter (*pAtABCG28*) and pollen tubes overexpressing *AtABCG28* under the *pLAT52* promoter.
(A) Time-series analysis of a growing pollen tube from an *atabcg28*/+ plant complemented with *pAtABCG28::mGFP4:gAtABCG28*.
(B) Time-series analysis of a growing pollen tube from an *atabcg28*/+ plant complemented with *pLAT52::EYFP:gAtABCG28*.
Note the accumulation and punctate distribution of AtABCG28 in the tips of the growing pollen tubes. (Scale bar, 5 μm.)

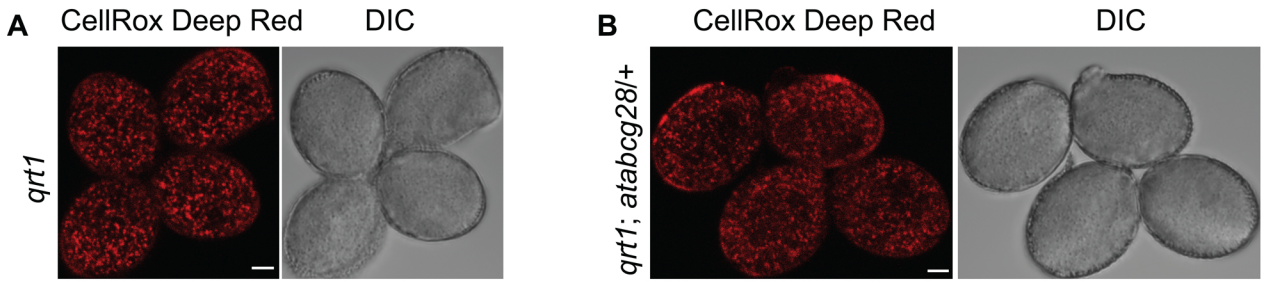

Figure S6. The hydroxyl radical and/or superoxide distribution in *atacbg28* pollen was not different from that in wild-type pollen. Hydroxyl radical and/or superoxide was detected using CellRox DeepRed dye.
(A) Hydroxyl radical and/or superoxide distribution in the early stages of *qrt1* tetrad germination.
(B) Hydroxyl radical and/or superoxide distribution in the early stages of *qrt1*; *atabcg28*/+ tetrad germination. The fluorescent signals from the four pollen are indistinguishable. (Scale bar, 5 μm.)

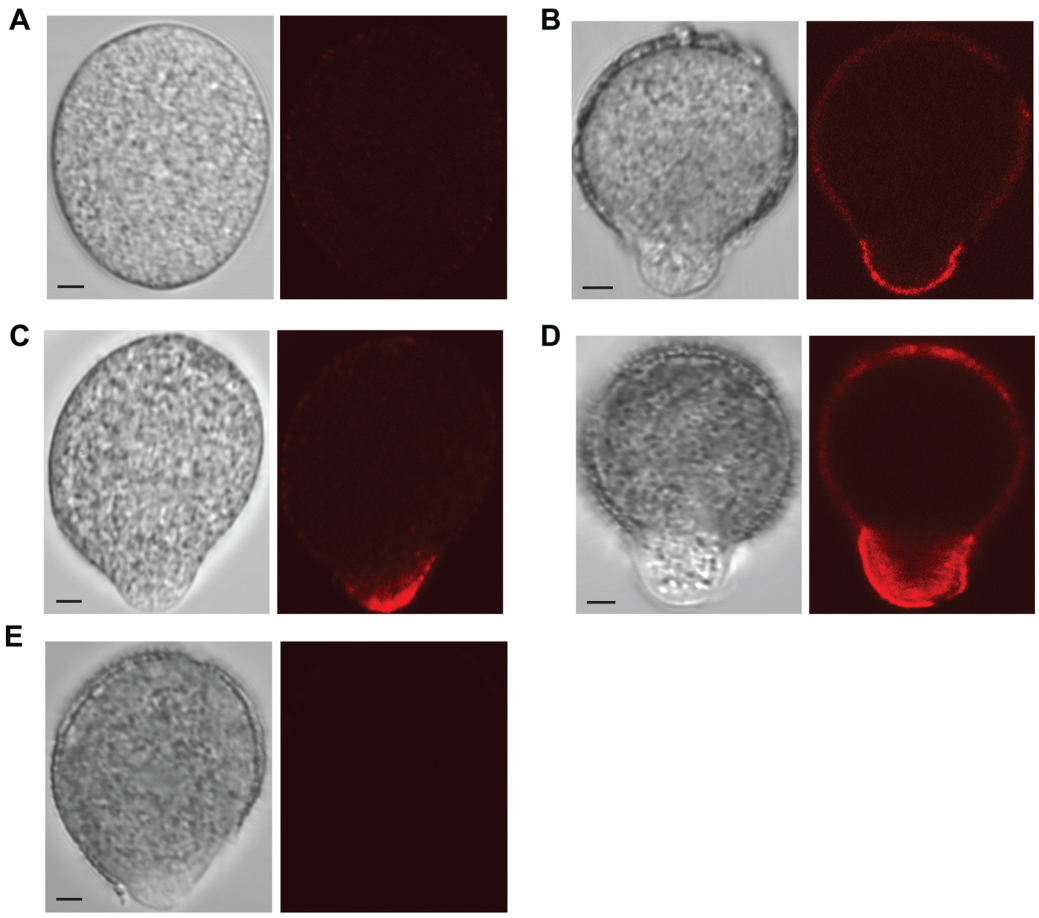

Figure S7. Polyamine is specifically localized to the tip of wild-type pollen tube.
Intracellular and apoplastic polyamines were labelled with anti-spermine/spermidine (Spm/Spd) antibody as the primary antibody and Alexa Fluor 568 Goat anti-Rabbit (IgG) antibody as the secondary antibody. Cell wall of the pollen was intact, or partially or thoroughly digested using pectinase and cellulase.
(A) When the cell wall was thoroughly digested, polyamines are not detected in non-germinating pollen grain.
(B) When the cell wall is not digested, polyamines are detected in the apoplast of the pollen tube.
(C) Polyamines are detected only in the cytosol of a pollen tube tip, but not in the grain, when the cell wall was thoroughly digested.
(D) Polyamines localize to both the apoplastic space and the cytosol of a pollen tube when the cell wall is partially digested. Cell wall digestion facilitated penetration of the Spm/Spd primary antibody into the cytosol.
(E) Autofluorescence from the negative control sample that was processed in the same way except for omitting the primary antibody.
(Scale bars, 2.5 μm.)

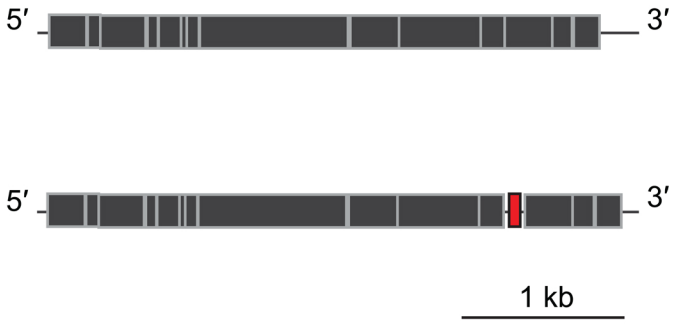

Parent	Self-fertilized progeny		n	Ratio	X^2	P value
	Sul ^{S} (+/+)	Sul ^{R} (*atabcg28*$^{-/+}$ and *atabcg28*$^{-/-}$)				
AtABCG28 transcript II in *atabcg28-1*$^{-/+}$	506	531	1037	1 : 1	0.04	> 0.05
AtABCG28 transcript II in *atabcg28-2*$^{-/+}$	473	574	1047	1 : 0.8	2.560	> 0.05

Figure S8. Arabidopsis plants express two forms of AtABCG28 transcript.
The base pair sequence of *AtABCG28* transcript I precisely matches the corresponding sequence in the Plant Membrane Protein Database (http://aramemnon.uni-koeln.de/). This transcript is found only in mature pollen grains and tubes, and we used a construct containing this sequence to ectopically express *AtABCG28* in the root hair (shown in Figure 7). Another *AtABCG28* transcript retaining the 11th intron (*AtABCG28* transcript II) is present in flower buds. This transcript encodes a truncated protein that lacks the 3rd–7th membrane-spanning domains (membrane domains shown in Figure 1) and failed to complement the fertility defect of *atabcg28*$^{-/+}$ (shown in this figure). P values > 0.05 indicate an insignificant difference from the 1:1 segregation ratio of transmission in *atabcg28*$^{-/+}$, calculated using a Chi-square test. Self-fertilized progeny of T2 generation *pLAT52:: AtABCG28* transcript II transgenic plants were used in this analysis. A total of 13 independent *atabcg28-1*$^{-/+}$ and 14 independent *atabcg28-2*$^{-/+}$ lines that expressed the alternatively spliced form of *AtABCG28* were tested and produced an identical result. Black boxes, exons; red box, intron. Sul ^{R}, sulfadiazine resistant; Sul ^{S}, sulfadiazine sensitive.

Figure S9. Site-directed mutagenesis to generate a stable *AtABCG28* coding sequence (CDS SDM).
Fifteen base pairs of the native full-length coding sequence of *AtABCG28* (from 1798 bp to 1812 bp) were often excised during replication in *E. coli*, possibly due to their propensity to form a hairpin structure. To prevent this, we introduced four sense mutations (red) into the sequence from 1798th to 1812th, a predicted site of hairpin formation.

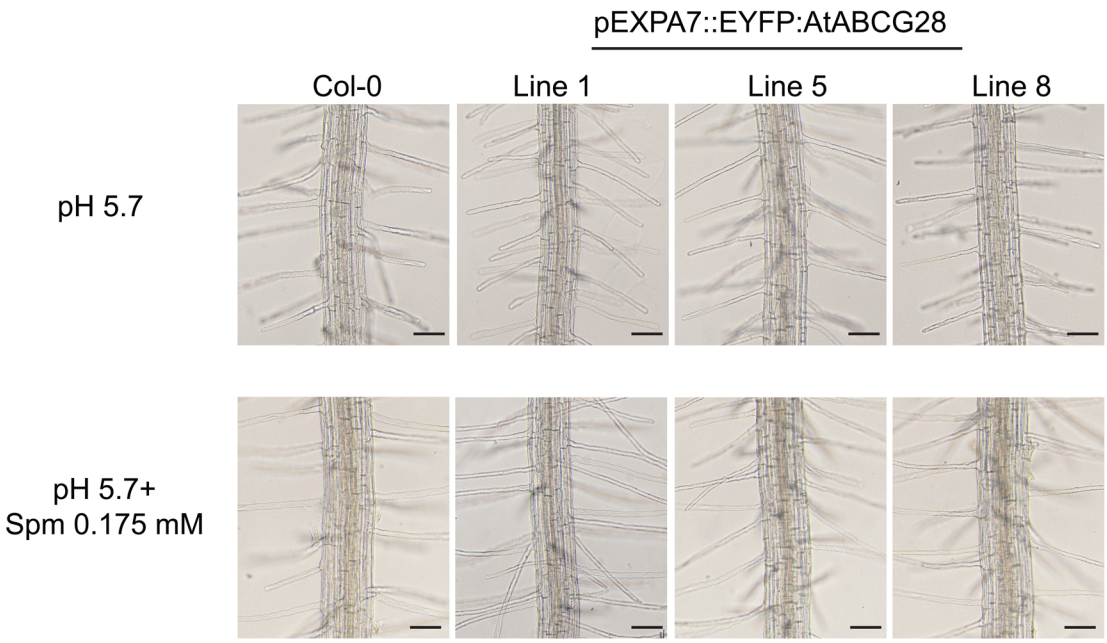

Figure S10. Root hairs expressing *AtABCG28* exhibit similar growth to that of the wild type under standard growth conditions.
Root hairs of transgenic plants that ectopically express *AtABCG28* exhibit similar growth to those of wild-type plants under standard growth conditions (pH 5.7) in the absence (top) or presence (bottom) of exogenous spermine (Spm) treatment. (Scale bars, 100 μm.)

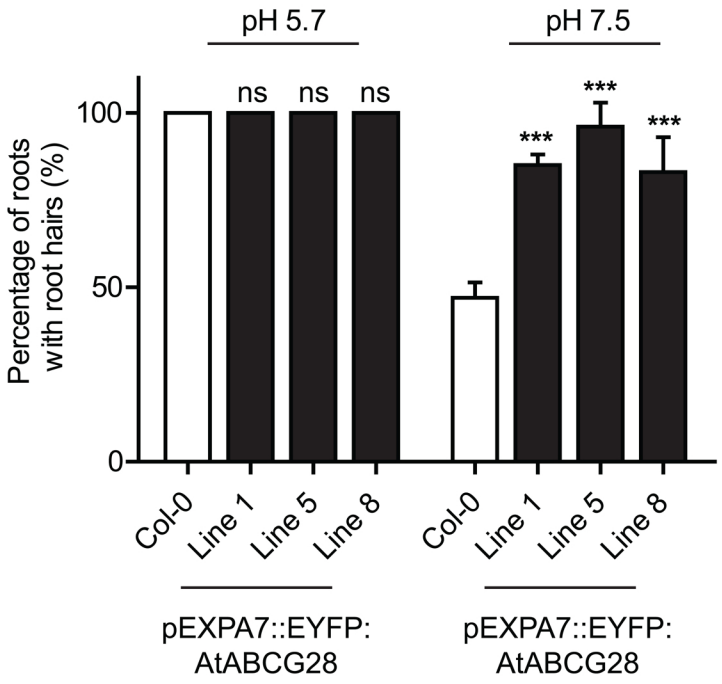

Figure S11. Ectopic expression of *AtABCG28* improves root hair growth at high pH. Percentage values of roots with hairs in normal pH (pH 5.7) and high pH (pH 7.5) conditions. Data were obtained from 50 to 100 roots per genotype in three independent experiments. Asterisks denote statistical significance between wild-type and transgenic plants, calculated by two-way ANOVA and Bonferroni post-tests (***, $p < 0.001$).

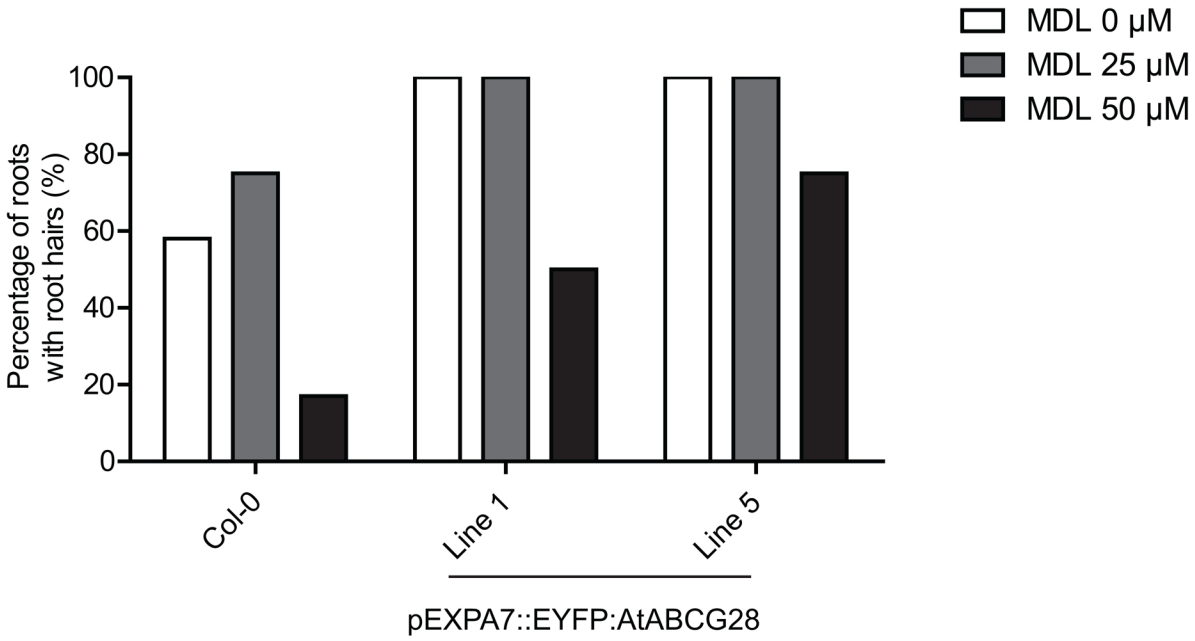

Figure S12. *AtABCG28*-mediated recovery of root hair growth at pH 7.5 depends on polyamines.
Treatment with a polyamine oxidase inhibitor (MDL 72527) substantially reduced the effect of AtABCG28 in promoting root hair growth at pH 7.5. This indicates that the recovery of root hair growth by AtABCG28 requires polyamine and its oxidation. Data were obtained from 30~40 roots per genotype.

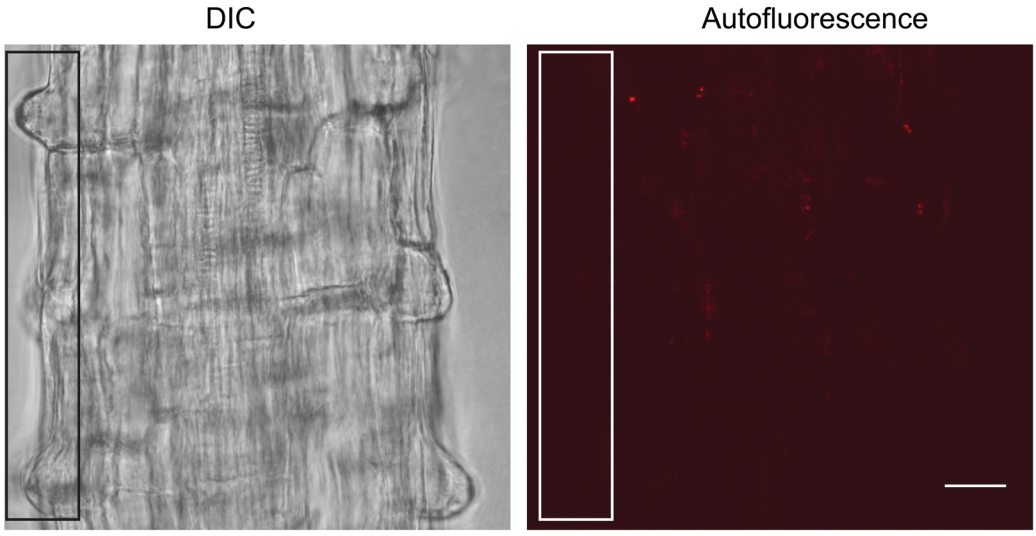

Figure S13. The epidermis of the root differentiation zone displayed no background autofluorescence.
Note that there was no fluorescence signal in the epidermis (boxed regions). Bright field (left) and fluorescence (right) images. Fluorescence image was obtained with excitation at 633 nm and emission at longer than 655 nm. (Scale bar, 10 μm.)

References

1. Kleinboelting N, Huep G, Kloetgen A, Viehoever P, & Weisshaar B (2012) GABI-Kat SimpleSearch: new features of the Arabidopsis thaliana T-DNA mutant database. Nucleic Acids Res.
2. Alonso JM*, et al.* (2003) Genome-wide insertional mutagenesis of Arabidopsis thaliana. *Science* 301(5633):653-657.
3. Preuss D, Rhee SY, & Davis RW (1994) Tetrad analysis possible in Arabidopsis with mutation of the QUARTET (QRT) genes. *Science* 264(5164):1458-1460.
4. Clough, S. J., & Bent, A. F. (1998). Floral dip: a simplified method for Agrobacterium-mediated transformation of Arabidopsis thaliana. *The Plant Journal*, *16*, 735-743.
5. Kim YY*, et al.* (2009) AtHMA1 contributes to the detoxification of excess Zn (II) in Arabidopsis. *The Plant Journal* 58(5):737-753.
6. Mizoi J, Nakamura M, & Nishida I (2006) Defects in CTP: PHOSPHORYLETHANOLAMINE CYTIDYLYLTRANSFERASE affect embryonic and postembryonic development in Arabidopsis. *The Plant Cell* 18(12):3370-3385.
7. Peterson R, Slovin JP, & Chen C (2010) A simplified method for differential staining of aborted and non-aborted pollen grains. *Int J Plant Biol* 1:e13.
8. Lee Y*, et al.* (2008) The Arabidopsis phosphatidylinositol 3-kinase is important for pollen development. *Plant physiology* 147(4):1886-1897.
9. Twell D, Yamaguchi J, Wing RA, Ushiba J, & McCormick S (1991) Promoter analysis of genes that are coordinately expressed during pollen development reveals pollen-specific enhancer sequences and shared regulatory elements. *Genes & development* 5(3):496-507.
10. Cho H-T & Cosgrove DJ (2002) Regulation of root hair initiation and expansin gene expression in Arabidopsis. *The Plant Cell* 14(12):3237-3253.
11. Lee Y*, et al.* (2008) Roles of phosphatidylinositol 3-kinase in root hair growth. *Plant physiology* 147(2):624-635.
12. Liu H & Naismith JH (2008) An efficient one-step site-directed deletion, insertion, single and multiple-site plasmid mutagenesis protocol. *BMC biotechnology* 8(1):91.

13. Vogler F, Konrad SS, & Sprunck S (2015) Knockin'on pollen's door: live cell imaging of early polarization events in germinating Arabidopsis pollen. *Frontiers in plant science* 6:246.
14. Schindelin J*, et al.* (2012) Fiji: an open-source platform for biological-image analysis. *Nature methods* 9(7):676.
15. Hwang J-U, Vernoud V, Szumlanski A, Nielsen E, & Yang Z (2008) A tip-localized RhoGAP controls cell polarity by globally inhibiting Rho GTPase at the cell apex. *Current Biology* 18(24):1907-1916.
16. Bock KW*, et al.* (2006) Integrating membrane transport with male gametophyte development and function through transcriptomics. *Plant Physiology* 140(4):1151-1168.